Research article

Reproducibility assessment of rapid strains in cardiac MRI: Insights and recommendations for clinical application

Moritz C. Halfmann [a,b], Luuk H.G.A. Hopman [c], Hermann Körperich [d], Edyta Blaszczyk [e,f], Jan Gröschel [e,f], Jeanette Schulz-Menger [e,f], Janek Salatzki [g,h], Florian André [g,h], Silke Friedrich [i], Tilman Emrich [a,b,*]

[a] Department of Diagnostic and Interventional Radiology, University Medical Center of the Johannes Gutenberg-University Mainz, Langenbeckstraße 1, 55131 Mainz, Germany
[b] German Center for Cardiovascular Research (DZHK), Partner Site Rhine-Main, Germany
[c] Department of Cardiology, Amsterdam UMC, Vrije Universiteit Amsterdam, Amsterdam Cardiovascular Sciences, De Boelelaan 1118, 1081 HV Amsterdam, the Netherlands
[d] Institute for Radiology, Nuclear Medicine and Molecular Imaging, Heart and Diabetes Center NRW, Ruhr-University of Bochum, 32545 Bad Oeynhausen, Germany
[e] Charité-Universitätsmedizin Berlin, corporate member of Freie Universität Berlin, Humboldt-Universität zu Berlin, and Berlin Institute of Health, Working Group on Cardiovascular Magnetic Resonance, Experimental and Clinical Research Center, a joint cooperation between the Charité Medical Faculty and the Max Delbrueck Center for Molecular Medicine, Lindenberger Weg 80, Berlin 13125, Germany
[f] German Center for Cardiovascular Research (DZHK), Partner Site, Berlin, Germany
[g] Department of Cardiology, Angiology, Pneumology, University Hospital Heidelberg, Im Neuenheimer Feld 410, 69121 Heidelberg, Germany
[h] German Center for Cardiovascular Research (DZHK), Partner Site Heidelberg-Mannheim, Germany
[i] Area19 Medical Inc., Montreal, Quebec, Canada

ARTICLE INFO

ABSTRACT

Purpose: Studies have shown the incremental value of strain imaging in various cardiac diseases. However, reproducibility and generalizability has remained an issue of concern. To overcome this, simplified algorithms such as rapid atrioventricular strains have been proposed. This multicenter study aimed to assess the reproducibility of rapid strains in a real-world setting and identify potential predictors for higher interobserver variation.
Methods: A total of 4 sites retrospectively identified 80 patients and 80 healthy controls who had undergone cardiac magnetic resonance imaging (CMR) at their respective centers using locally available scanners with respective field strengths and imaging protocols. Strain and volumetric parameters were measured at each site and then independently re-evaluated by a blinded core lab. Intraclass correlation coefficients (ICC) and Bland-Altman plots were used to assess inter-observer agreement. In addition, backward multiple linear regression analysis was performed to identify predictors for higher inter-observer variation.
Results: There was excellent agreement between sites in feature-tracking and rapid strain values (ICC $\geq$ 0.96). Bland-Altman plots showed no significant bias. Bi-atrial feature-tracking and rapid strains showed equally excellent agreement (ICC $\geq$ 0.96) but broader limits of agreement ($\leq$18.0 % vs. $\leq$3.5 %). Regression analysis showed that higher field strength and lower temporal resolution ($>$30 ms) independently predicted reduced interobserver agreement for bi-atrial strain parameters (ß = 0.38, p = 0.02 for field strength and ß = 0.34, p = 0.02 for temporal resolution).

Conclusion: Simplified rapid left ventricular and bi-atrial strain parameters can be reliably applied in a real-world multicenter setting. Due to the results of the regression analysis, a minimum temporal resolution of 30 ms is recommended when assessing atrial deformation.

1. Introduction

In the last decade, multiple studies have proven the incremental value of strain imaging in comparison to long-established parameters such as ejection fraction (EF) or the presence of focal fibrosis regarding prognosis in various cardiac diseases [1–5]. However, reproducibility and generalizability of strain imaging has remained an issue of concern.

Since the implementation of post-processing approaches for echocardiography [6] and later feature-tracking strain for cardiac magnetic resonance imaging (cardiac MRI) [7–9], multiple studies have evaluated differences between modalities as well as software solutions [10–12]. In addition, research has also aimed at identifying potential confounding factors in specific diseases [13] and at defining optimal temporal and spatial resolution [14] for feature-tracking strain measurements. However, contrary to these efforts, commercial vendors still blind their users to the details of their algorithms, virtually creating black-box models [7]. This has prompted efforts to simplify the algorithms to make them more comprehensible. Recently, rapid strain approaches have been introduced as alternatives to conventional feature-tracking strains for the assessment of deformation patterns in different cardiomyopathies.

Rather than tracking the tissue of the myocardial wall over time, this method calculates longitudinal shortening of both atria and the left ventricle (LV) in relation to the atrioventricular valve planes. To do so, it does not require specialized post-processing software nor does it require significant amounts of processing power, making it a simple and fast alternative for cardiac function assessment of the LV and atria.

After these were initially only used as research tools, they were more recently adopted in clinical software solutions. While previous studies have made efforts to evaluate reproducibility, they often focused on imaging protocols in a research context [15,16], thereby not taking the potential impact of different scanner types and acquisition protocols into account. Therefore, this study aimed to assess the reproducibility of simplified ventricular and bi-atrial cardiac MRI strain parameters in a real-world, multicenter setting and to identify factors causing measuring variations.

2. Materials and methods

The agreement of cardiac MRI rapid strain measurements was assessed in a multicenter, multi-vendor trial. Locally responsible institutional ethics committees approved the study protocol, which was in line with the Declaration of Helsinki with a waiver for informed consent.

2.1. Study population

Each of the four participating sites retrospectively identified 20 patients and 20 healthy controls (HC) of a local examined/assessable cohort. Inclusion criteria for the patient populations were clinical indication for cardiac MRI with pathological findings. Clinical records, including additional diagnostics tests, subsequently verified the diagnosis. For cross-center analyses, patients were grouped by three morphological disease phenotypes: hypertrophic, dilated and indistinct.

Inclusion criteria for the HC were no history, signs or symptoms of cardiac diseases, no cardiovascular risk factors (e.g., hypertension or diabetes), and normal left and right ventricular function according to institutional reference ranges.

2.2. Cardiac MRI acquisition

The minimum requirement for all imaging protocols was the use of a retrospectively gated standard balanced steady-state free precession (bSSFP) sequence for cine imaging. Short-axis stacks completely covering both the left and right ventricle and standardized cardiac long axis views (2-, 3- and 4- chamber) were mandatory. Compressed-sensing sequences as well as studies with artefacts (wrap around, respiratory/cardiac ghosting, image blurring/mistriggering, metallic artefacts, shimming artefacts or signal loss [17]) were excluded from this study according to the study's prospectively drafted standard operating procedures (SOP).

2.3. Image analysis

Prior to the segmentation of the datasets, all sites were given an SOP for volumetric and strain measurements, the core lab had drafted. Then, one observer from each site performed LV, left atrial (LA), and right atrial (RA) volumetric analysis on all 40 subjects by manually correcting the AI-derived end-diastolic and end-systolic contours in the 2- and 4-chamber long-axis views as well as the short-axis stacks, carefully excluding the left ventricular outflow tract and papillary muscles. All observers had a minimum of 5 years of experience in cardiovascular imaging (site 1: 5 years, site 2: 23 years of experience, site 3: 8 years, site 4: 6 years). All measurements were performed using dedicated software (cvi42, version 5.13.2, Circle Cardiovascular Imaging Inc., Calgary, Canada).

Rapid LV strain was calculated by measuring the relative longitudinal shortening of the distance between the atrioventricular junction and the apex. This method involved assessing the changes in length along the longitudinal axis of the left ventricle during the cardiac cycle. Similarly, rapid bi-atrial strains were measured by assessing the relative longitudinal shortening and extension of the distance between the atrioventricular junction and the apex of both atria. LV and LA results were averaged from both long axes according to the biplane-area length method [18], while RA results were derived only from the 4-chamber view. Additionally, feature-tracking global longitudinal strain (GLS) analysis was performed using all long-axis sequences, while the previously manually corrected AI-derived contours were not modified. A clinical example of both feature-tracking and rapid strain analysis can be seen in Fig. 1.

After analysis by the local site observers and contours were deleted, the core lab observer (***blinded for peer review***, 6 years of experience) then re-evaluated all 160 studies by either traveling to the site (sites 2 and 4) or remotely accessing the studies (sites 1 and 3). The core lab did not provide data for this study to prevent bias.

2.4. Statistical analysis

Statistical analysis was performed using dedicated software (SPSS Statistics for Windows; v23.0; IBM Corp Armonk, NY, USA).

The Shapiro-Wilk test was used to assess the normal distribution of continuous data. Continuous data are either expressed as mean $\pm$ standard deviation (SD) or as with median with interquartile range (Q1, Q3), as appropriate. Categorical data are expressed as numbers and proportions. As strain values relate to an end-diastolic reference frame, the values for atrial strain are positive (atrial expansion during systole) while ventricular strain values are negative (ventricular shortening during systole).To evaluate the interobserver agreement between the site and the core lab, two-way random-effects model intraclass correlation coefficients (ICC) and Bland-Altman plots were used. For the Bland-Altman analyses were performed with the core lab measurements as the reference standard, differences of the means were calculated by

subtracting the sites' means from the core lab's means and limits of agreement (LoA) were found by 95 % confidence intervals of the mean difference (1.96 × SD). Levels of agreement were defined as follows: poor, <0.5; moderate, 0.5–0.75; strong, 0.76–0.9; excellent, >0.9 [19].

Differences between site observers' and core lab results were evaluated by paired t-tests. The interobserver variation was determined per subject by dividing the mean absolute difference of the strain values (pooled sites-core lab) by the mean value of all observers for the respective parameters. The results were classified as: low (<10 %); intermediate (11–20 %); high (21–30 %); and very high (>30 %) [20].

The predictive value of influencing factors on the interobserver variation was assessed by multiple regression analysis with backward elimination. Variables entered into the regression analysis were the MRI scanner vendor, magnetic field strength, phases per cardiac cycle, type of core lab evaluation (on-site visit/remote access), heart rate, and temporal resolution. The latter was calculated per subject by dividing the RR-Interval by the acquired phases per cardiac cycle.

To control for the different diagnoses as potential confounding variables, subjects were classified into four morphological groups as follows: (I) hypertrophic disease phenotype (hypertrophic cardiomyopathy (HCM), amyloidosis), (II) dilated disease phenotype (dilated cardiomyopathy (DCM)), (III) other disease phenotypes (e.g. myocarditis), (IV) healthy controls. The analyses were performed per group and results

were compared between pooled site observers and the core lab. A two-sided p-value <0.05 was considered statistically significant.

3. Results

3.1. Baseline characteristics and acquisition parameters

Each participating site contributed data from 20 patients and 20 HC, resulting in a total of 160 subjects (median 49 (18 to 85) years; 64 (40 %) females). The patient cohort included 38 (48 %) patients with a hypertrophic disease phenotype (11 patients with amyloidosis, 27 patients with HCM), 30 (38 %) patients with a dilated disease phenotype, and 12 (14 %) with an indistinct disease phenotype (7 with ischemic cardiomyopathy, 5 patients with acute myocarditis). Detailed baseline characteristics for all sites are provided in Table 1.

All patients and HC had undergone cardiac MRI at their respective centers using locally available scanners from two manufacturers (Siemens Healthcare; Philips Healthcare) with either 1.5 T (sites 1, 3 and 4) or 3 T (sites 2 and 4). Key acquisition parameters for all sites can be found in Table 2.
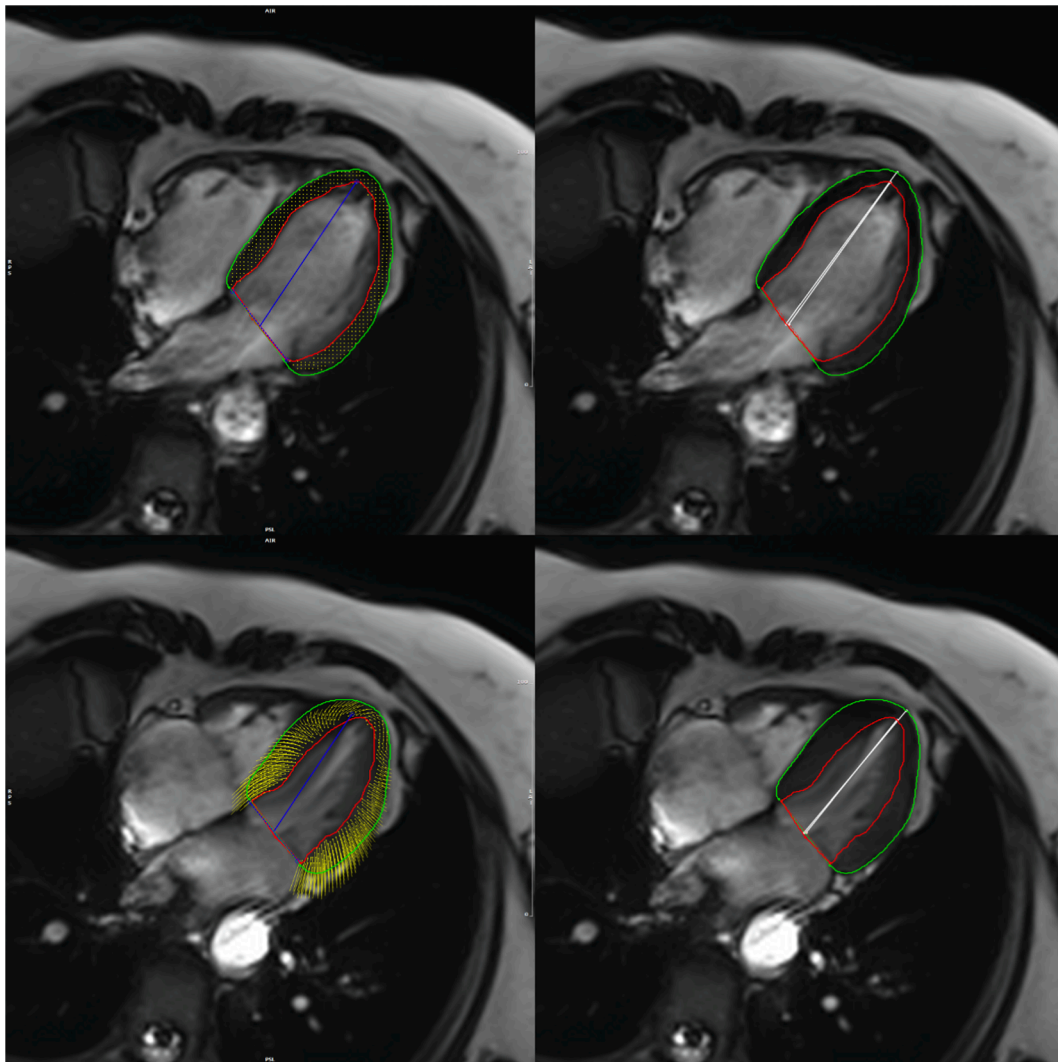
Fig. 1. Clinical example of a four-chamber view bSSFP cine sequence from a 71 year old female healthy volunteer. The top row shows images from the end-diastolic phase while the bottom row shows images from the end-systolic phase. Feature-tracking GLS can be seen on the left with myocardial tracking points (yellow) and rapid strain contours are shown on the right (white line marks longitudinal extend between apex and atrioventricular valve plane).

Table 1
Baseline characteristics for each site.

	1	2	3	4
Study population				
Amyloidosis	0 (0)	7 (18)	4 (10)	0 (0)
DCM	20 (50)	0 (0)	0 (0)	10 (25)
HCM	0 (0)	13 (32)	4 (10)	10 (25)
Ischemic	0 (0)	0 (0)	7 (17)	0 (0)
Myocarditis	0 (0)	0 (0)	5 (13)	0 (0)
HC	20 (50)	20 (50)	20 (50)	20 (50)
Study characteristics				
Female (%)	17 (43)	16 (40)	11 (28)	20 (50)
Age (years)	51 ± 15	49 ± 13	47 ± 18	49 ± 13
Weight (kg)	79.3 ± 15.1	75.4 ± 13.4	74.0 ± 13.0	76.3 ± 14.3
Height (cm)	174.9 ± 9.1	172.7 ± 11.3	176.5 ± 7.7	173.9 ± 9.9
BMI (kg/m^2)	27.0 ± 5.0	25.2 ± 3.2	23.8 ± 3.5	25.0 ± 3.0
BSA (m^2)	1.99 ± 0.21	1.90 ± 0.22	1.90 ± 0.19	1.91 ± 0.22
HR (1/min)	70.0 ± 12.0	65.8 ± 8.7	73.6 ± 14.3	67.0 ± 9.0

Continuous parameters are expressed as mean ± standard deviation.
1, ***blinded for peer review***; 2, ***blinded for peer review***; 3, ***blinded for peer review***; 4, ***blinded for peer review***.

Table 2
Key acquisition parameters for each site.

	1	2	3	4
Site				
Site	***blinded for peer review***	***blinded for peer review***	***blinded for peer review***	***blinded for peer review***
Country	***blinded for peer review***	***blinded for peer review***	***blinded for peer review***	***blinded for peer review***
Scanner				
Vendor	Siemens	Philips	Siemens	Philips
Type	Avanto/Sonata	Achieva	Avanto	Ingenia CX/Ingenia
Field strength (T)	1.5	3	1.5	1.5 (27)/3 (13)
Core lab evaluation	remote	on-site	remote	on-site
Acquisition parameters				
TR (ms)	2.4	2.7	3.9	3.0/4.0
TE (ms)	1.57	1.35	1.20	1.48/2.0
Phases/cardiac cycle	20	45	30	35
Temporal resolution (ms)	44.2 ± 7.5	20.6 ± 2.4	28.1 ± 5.3	26.4 ± 3.7
Flip angle (°)	60	42	70	60/45
Slice thickness (mm)	6.0	6.0	6.0	8.0
Slice gap	0	0	0	0
FOV (mm)	266 × 340	250 × 270	340 × 360	350 × 350/320 × 320
Contrast usage	yes	yes	yes	yes

Continuous parameters are expressed as mean ± standard deviation.

3.2. Interobserver agreement

Overall, there was excellent agreement for LV parameters, including rapid strain between site observers and the core lab (ICC ≥ 0.96). In addition, there were no significant differences between the site observers' results and the core lab evaluation for both LV volumetric and LV strain parameters (Fig. 2).

In addition, a strong-to-excellent agreement was also observed for bi-atrial volumetric and junctional strain parameters (LA: ICC ≥ 0.93; RA: ICC ≥ 0.89) and there were no significant differences between the site observers' results and the core lab (Fig. 3). In further analysis, Bland-Altman plots (Fig. 4) revealed no systematic bias for ventricular or atrial strain parameters (mean differences all ≤±1.2 %), but the LoA were broader for atrial rapid strains compared to ventricular rapid strains and feature-tracking GLS (LoA ≤ 18.0 % vs. ≤3.5 %). Detailed results of the interobserver agreement between pooled site observers and the core lab are given in Table 3.

3.3. Analysis per site

In the site-specific analysis, the overall results were mostly confirmed. All volumetric LV parameters showed excellent agreement between site observers and the core lab (ICC ≥ 0.91), except for EF at site 2, which showed strong agreement (ICC 0.79). Both feature-tracking GLS and LV rapid strain showed excellent agreement (ICC ≥ 0.92). Detailed results of the interobserver agreement of LV parameters per site are given in Supplemental Table S1.

LA volumetric parameters showed excellent agreement between site observers and the core lab (ICC ≥ 0.95), while RA volumetric parameters showed strong-to-excellent agreement (ICC ≥ 0.83). Both LA and RA feature-tracking and rapid strains demonstrated strong-to-excellent agreement (ICC ≥ 0.82). Detailed results of the interobserver agreement of bi-atrial parameters per site can be found in Supplemental Table S2.

3.4. Analysis per cohort

In the analysis based on morphological groups, the pooled results of the site observers and the core lab revealed strong-to-excellent agreement for LV volumetric values and all strain parameters for the 38 patients with a hypertrophic disease phenotype (ICC ≥ 0.89), excellent agreement for the 30 patients with a dilated disease phenotype (ICC ≥ 0.90) and excellent agreement for the remaining 12 patients with other morphological disease phenotypes (ICC ≥ 0.90). The cohort of 80 healthy controls showed strong-to-excellent interobserver agreement (ICC ≥ 0.81). Detailed results of the interobserver agreement of all LV parameters per cohort can be found in Supplemental Table S3.

Further, the bi-atrial measurements showed excellent agreement for volumetric and strain parameters within the patients with a hypertrophic disease phenotype (ICC ≥ 0.96), strong-to-excellent agreement in patients with a dilated disease phenotype (ICC ≥ 0.88), and strong-to-excellent agreement for the patients with an indistinct morphological disease phenotype (ICC ≥ 0.81). In the healthy controls, the agreement for RA volumetric and strain parameters was moderate-to-strong (ICC ≥ 0.68) while LA parameters showed strong-to-excellent interobserver agreement (ICC ≥ 0.89). Detailed results of the interobserver agreement of bi-atrial parameters per cohort can be found in Supplemental Table S4.

3.5. Interobserver variation

Overall, the interobserver variation of ventricular strain measurements between the site observers and the core lab was at 7.7 % while the interobserver variation of bi-atrial measurements was slightly larger at 10.6 %. In the analysis per site, the largest interobserver variation for ventricular strain parameters was found for site 1 and the smallest for site 4 (13.1 % vs. 5.4 %). This observation was confirmed in bi-atrial strain measurements (18.9 % vs. 6.0 %). In the analysis per morphological disease phenotype, healthy controls had the lowest interobserver variation between pooled sites and the core lab for all strain parameters (6.0 % for ventricular and 6.9 % for bi-atrial strain), whereas the indistinct disease phenotype showed the largest interobserver variation for ventricular strain (20.7 %) and the dilated disease phenotype showed the largest interobserver variation for bi-atrial (23.3 %). Detailed results for all analyses of interobserver variation are given in Table 4.

The regression analysis was performed on healthy controls to minimize bias. For ventricular strain parameters, a 5-step model did not show
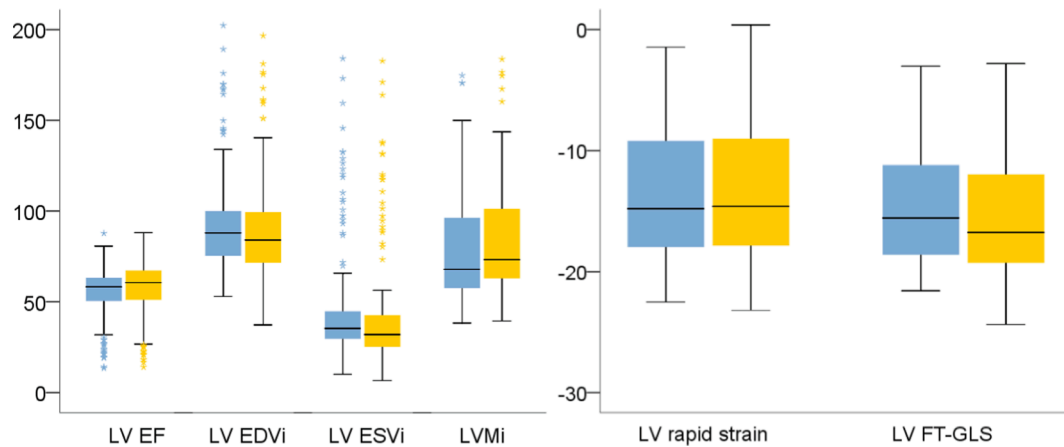
Fig. 2. Boxplots comparing the site observers' results (blue boxes) and the core lab results (orange boxes) for volumetric LV parameters (left) and LV strain parameters (right).
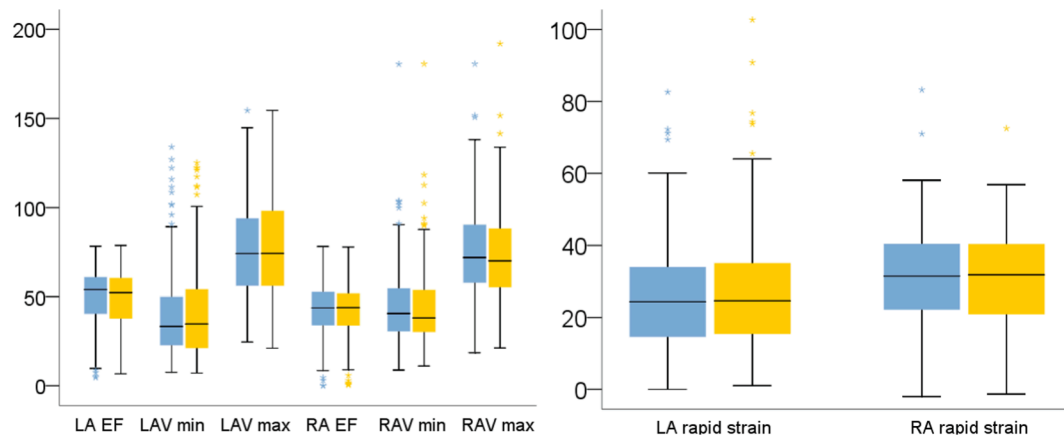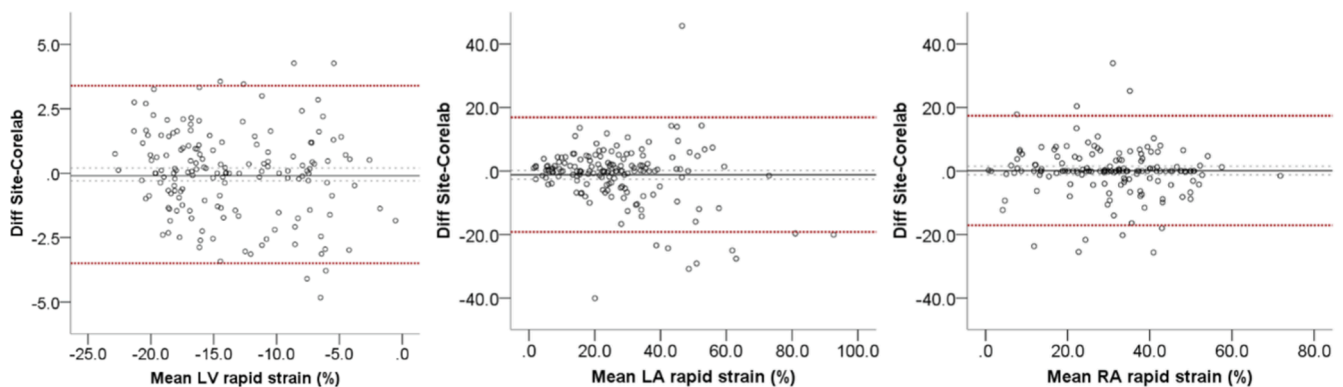

Fig. 3. Boxplots comparing the site observers' results (blue boxes) and the core lab results (orange boxes) for volumetric bi-atrial parameters (left) and bi-atrial strain parameters (right).

Fig. 4. Bland-Altman plots showing the agreement between the site observers' results and the core lab for LV rapid strain (left), LA rapid strain (middle), and RA rapid strain (right). Note that the scales for ventricular and atrial strains are different due to differences in limits of agreement.

a significant influence of scanner type, field strength, phases per cardiac cycle, heart rate, or temporal resolution on the interobserver variation. For atrial strain parameters however, a 4-step model revealed that a higher field strength and lower temporal resolution had a significant predictive value for higher interobserver variation (ß = 0.38, p = 0.02 for field strength and ß = 0.34, p = 0.02 for temporal resolution). Of note, temporal resolution was eliminated from the prediction model when performing the regression analysis of this study only on the sites

with a mean temporal resolution > 30 ms (sites 2–4). Detailed results of both regression analyses are summarized in Table 5.

4. Discussion

This multicenter study aimed to assess agreement of simplified junctional left ventricular and bi-atrial strain parameters between different observers, scanner types, field strengths and sites. This was

Table 3
Interobserver agreement over all parameters and cohorts.

	Sites	Core Lab	Diff (%)	LoA (%)	ICC	Interobs. Var. (%)
LV EF (%)	59.1 (51.1, 64.5)	61.2 (53.7, 68.2)	−2.7	11.9	0.96	6.6
LV EDVi (ml/m^2)	88.0 (75.3, 100.1)	84.1 (71.6, 100.1)	2.7	10.1	0.99	3.0
LV ESVi (ml/m^2)	35.3 (29.4, 44.8)	32.0 (25.0, 43.3)	3.3	10.5	0.99	8.6
LVMi (g/m^2)	67.9 (57.4, 96.9)	73.3 (62.6, 101.4)	−5.1	13.3	0.99	6.5
LV rapid strain (%)	−14.8 (-18.0, −9.2)	−14.7 (-17.9, −9.0)	−0.1	3.5	0.97	7.6
LV FT-GLS (%)	−15.6 (-18.6, −11.1)	−16.8 (-19.3, −11.9)	0.8	3.4	0.97	7.1
LA EF (%)	54.0 (40.2, 61.4)	52.3 (37.7, 60.5)	1.2	12.9	0.96	5.6
LAV min (ml)	33.2 (22.4, 50.0)	34.5 (21.1, 57)	−1.0	14.2	0.98	6.9
LAV max (ml)	73.9 (56.0, 94.2)	74.0 (56.0, 98.2)	0.8	12.6	0.99	2.9
RA EF (%)	44.1 (34.1, 53.2)	43.1 (33.8, 51.8)	1.5	19.8	0.89	9.4
RAV min (ml)	39.9 (30.5, 54.6)	38.7 (30.4, 53.9)	−0.2	15.1	0.97	4.6
RAV max (ml)	72.0 (57.8, 90.4)	70.3 (55.2, 88.5)	2.0	18.5	0.97	3.5
LA rapid strain (%)	24.6 (14.6, 34.0)	24.8 (15.4, 36.3)	−1.2	18.0	0.93	18.1
RA rapid strain (%)	31.8 (22.2, 40.5)	31.8 (20.8, 40.5)	0.1	17.2	0.89	8.4

Diff, mean difference; LoA, limits of agreement; ICC, intraclass correlation coefficient; Interobs. Var., interobserver variation (mean absolute difference ÷ mean); LV, left ventricular; EF, ejection fraction; EDVi, end-diastolic volume index; ESVi, end-systolic volume index; LVMi, left ventricular mass index; MAPSE, mitral annular plane systolic excursion; FT-GLS, feature-tracking global longitudinal strain.
Continuous parameters are expressed as median with interquartile range (Q1, Q3).

Table 4
Variation of Strain Parameters Over All Subjects per Site and per Cohort.

	n	Interobserver Variation (%)
Ventricular Strain		
Overall	160	7.7 (2.7, 16.1)
Site 1	40	13.1 (6.1, 27.3)
Site 2	40	5.9 (1.7, 11.5)
Site 3	40	7.4 (3.0, 15.4)
Site 4	40	5.4 (1.5, 15.2)
Cohorts		
Hypertrophic	38	5.8 (1.4, 23.6)
Dilated	30	18.0 (7.1, 35.6)
Indistinct	12	20.7 (2.7, 54.1)
Healthy	80	6.0 (2.1, 10.7)
Bi-Atrial Strain		
Overall	160	10.6 (2.2, 22.2)
Site 1	40	18.9 (6.2, 34.8)
Site 2	40	11.9 (1.0, 23.2)
Site 3	40	8.0 (3.2, 13.6)
Site 4	40	6.0 (0.0, 20.9)
Cohorts		
Hypertrophic	38	11.3 (0.3, 19.9)
Dilated	30	23.3 (8.1, 35.3)
Indistinct	12	17.7 (6.9, 37.0)
Healthy	80	6.9 (1.7, 16.8)

Continuous parameters are expressed as medians with interquartile range (Q1, Q3).

Table 5
Stepwise Backward Regression Analysis for Interobserver Variation.

	Ventricular Strain		Bi-atrial Strain	
	ß	p-value	ß	p-value
Step 1				
Type of core lab analysis	0.00	0.99	0.00	0.99
Scanner vendor	−0.03	0.90	0.07	0.73
Field strength (T)	−0.23	0.29	0.44	**0.06**
Phases per cardiac cycle	0.29	0.61	−0.32	0.87
Heart rate (1/min)	−0.04	0.87	−0.17	0.76
Temporal resolution (ms)	0.30	0.54	0.23	0.63
Step 2				
Scanner vendor	–	–	0.06	0.75
Field strength (T)	−0.23	0.28	0.37	**0.02**
Phases per cardiac cycle	0.27	0.62	–	–
Heart rate (1/min)	0.05	0.84	−0.04	0.80
Temporal resolution (ms)	0.31	0.54	0.30	0.16
Step 3				
Scanner vendor	–	–	0.09	0.57
Field strength (T)	−0.22	0.28	0.38	**0.02**
Phases per cardiac cycle	0.19	0.58	–	–
Temporal resolution (ms)	0.22	0.37	0.34	**0.02**
Step 4				
Scanner vendor	–	–	0.09	0.57
Field strength (T)	−0.13	0.31	0.38	**0.02**
Temporal resolution (ms)	0.11	0.43	0.34	**0.02**
Step 5				
Field strength (T)	−0.19	0.10	n/a	n/a

Backward elimination criterion: Probability of F-to-remove ≥0.05.
Significant predictors are highlighted in bold.

accomplished by including 160 subjects (80 patients with various cardiac diseases and 80 healthy controls) from 4 different sites.

The main results are: (I) Rapid LV and bi-atrial strain parameters showed strong-to-excellent interobserver agreement (II) LV strain parameters showed low interobserver variability while bi-atrial parameters showed intermediate interobserver variability (III) higher field strength as well as lower temporal resolution were associated with higher interobserver variation in bi-atrial strain measurements.

Despite most commercially available software solutions relying on feature-tracking methods, significant inter-vendor differences have been demonstrated for ventricular [10] as well as atrial strain measurements [12]. In the absence of free access to vendor-specific algorithms, differences between them often get lost in the 'black box' [7] and simplified strain algorithms have been proposed [15,16]. These require far less sophisticated algorithms and can therefore potentially be more easily implemented by different vendors. In addition, they are also less demanding than feature-tracking algorithms in terms of manual corrections and quality assurance needed by the radiologist.

4.1. Ventricular parameters

After the adaptation of these research tools into commercial software, previous single-center studies on ventricular strain parameters found no significant bias for different field strengths [21] and demonstrated non-inferiority compared to feature-tracking strain [16]. These results were confirmed in the present study, despite this multicenter study showing a larger degree of interobserver variation in the setting compared to the single center setting (7.6 % vs. 3.4 % [16]). Of note, the interobserver variation for all ventricular functional and volumetric parameters such as LV EF and LV end-systolic volume index (ESVi) as well as the feature-tracking strain were similarly low (<10 %).

In the analysis per participating center, site 2 showed lower reproducibility of LV EF due to differences in LV ESVi. Ventricular strain and bi-atrial volumetric and strain parameters however were unaffected and showed excellent reproducibility. The most likely explanations for this could be the greater prevalence of LV hypertrophy in the patient cohort of this center compared to the others, resulting in more manual corrections needed for the endocardial end-systolic contours. In a similar

fashion, the hypertrophy could have also led to differences in contouring of trabeculations in these contours. The fact that the strain values were less affected by this can be explained by the algorithm, which prioritizes end-diastolic over end-systolic contours in order to compute strain. The regression analysis did not show a significant influence of the type of core lab analysis (on-site visit/remote access), scanner vendor, field strength, phases per cardiac cycle, heart rate, or temporal resolution. Thus, the results of this multi-center study corroborate previous single-center studies in finding that simplified ventricular rapid strain parameters can be reliably performed in a real-world setting [15,16,21].

4.2. Atrial parameters

Despite broad agreement on the potential that quantification of atrial function and deformation offers in terms of diastolic assessment and prognostic implications in various diseases [22–25], it currently remains a research tool. There are several reasons for this, such as the thin atrial walls complicating the contouring of the atrium and anatomical difficulties like the orifices of the pulmonary veins and atrial appendages impairing feature-tracking [26,27].

Similarly, to previous studies on simplified LA strain parameters, this study demonstrated no significant inter-observer bias [26]. However, the LoA were much broader than previously published. The most likely explanation for this is the more diverse cohort of patients compared to a rather homogenous cohort of heart failure patients in prior trials [26]. Interestingly, there were no relevant differences between volumetric and strain parameters. The interobserver variations were low (<10 %) for all LA volumetric parameters as well as all RA strain and volumetric parameters but intermediate for LA rapid strain. This superior reproducibility of the RA rapid strains compared to LA rapid strains is especially noteworthy because all RA parameters were only derived from the 4-chamber long-axis view, while LA parameters were averaged from 4-chamber and 2-chamber long-axis views. The most likely explanation for this is that the averaging not only adds another datapoint for more accurate anatomical representation of the LA but also adds an additional layer of potential measurement variations.

Previous studies have found superior interobserver agreement for right ventricular strain at lower field strengths [13]. Despite the higher spatial resolution at 3 T which would suggest superior tracking, it is also known that image artifacts such as pulsatile flow artifacts are typically more pronounced at higher field strengths. This potential cause of maltracking is further aggravated because cardiac MRI acquisition are commonly centered around ventricular assessment and sophisticated post-processing techniques are not routinely applied to the atria. Therefore, in this real-world scenario, flow artifacts which did not inhibit visual assessment of the atria might have been tolerated at the time of acquisition but hampered strain assessment nevertheless. This hypothesis is further supported by the fact, that ventricular strain assessment was not significantly confounded by higher field strength.

In terms of temporal resolution as a confounding factor of interobserver reproducibility, however, the available literature is inconsistent. While Fischer et al. [13] did not report temporal resolution as a relevant confounding factor, Backhaus et al. [14] found that higher temporal resolution lead to better reproducibility for right ventricular strain parameters. While the transferability of these results to atrial strain measurements remains unclear, the possible reasons for the influence of the temporal resolution can be transferred to strain measurements in general. These include improved tracking quality due to smaller magnitudes of movement within the smaller time frames between phases and less need for extrapolation between the data points [14]. Accordingly, when performing the regression analysis of this study only on the sites with a mean temporal resolution < 30 ms (sites 2–4), the temporal resolution was eliminated from the backward regression model at the first step. Based on these results, it is recommended to acquire the cine sequences with a minimum temporal resolution of 30 ms.

4.3. Limitations

First, only one post-processing software was used for strain measurements. In addition, due to its more complex contraction pattern, the right ventricular strain could not be semi-automatically assessed by the simplified strain algorithm and was therefore beyond the scope of this study.

Second, only adult subjects were included, so transferability to children remains to be determined. Lastly, because all sites routinely used intravascular contrast agents, this effect on strain quantification could not be studied.

5. Conclusion

Simplified left ventricular and bi-atrial strain parameters show strong-to-excellent agreement in a real-world multi-center setting, despite different scanner vendors, field strengths, and imaging protocols. Higher field strength and lower temporal resolution were independently associated with higher interobserver variation in bi-atrial strain measurements. When assessing atrial deformation, it is recommended to acquire the underlying cine sequences with a minimum temporal resolution of 30 ms.

CRediT authorship contribution statement

Moritz C. Halfmann: Investigation, Formal analysis, Data curation. **Luuk H.G.A. Hopman:** Investigation, Formal analysis, Writing – review & editing. **Hermann Körperich:** Investigation, Formal analysis. **Edyta Blaszczyk:** Investigation, Formal analysis. **Jan Gröschel:** Writing – review & editing, Formal analysis. **Jeanette Schulz-Menger:** Writing – review & editing, Supervision, Resources. **Janek Salatzki:** Investigation, Formal analysis. **Florian André:** Writing – review & editing, Visualization, Validation, Methodology. **Silke Friedrich:** Writing – review & editing, Supervision, Project administration, Conceptualization. **Tilman Emrich:** Writing – review & editing, Visualization, Supervision, Project administration, Conceptualization.

Declaration of competing interest

The authors declare the following financial interests/personal relationships which may be considered as potential competing interests: 'TE has received a speaker fee and travel support from Siemens Healthineers. SF is a former employee and stakeholder of Circle Cardiovascular Imaging. AF has received research support from Philips Healthcare, Siemens Healthcare and Circle Cardiovascular Imaging. None of these companies directly supported this study and none of the other authors report a conflict of interest'.

Appendix A. Supplementary material

Supplementary material to this article can be found online at https://doi.org/10.1016/j.ejrad.2024.111386.

References

[1] F. Frojdh, Y. Fridman, P. Bering, A. Sayeed, M. Maanja, L. Niklasson, E. Olausson, H. Pi, A. Azeem, T.C. Wong, P. Kellman, B. Feingold, A. Christopher, M. Fukui, J. L. Cavalcante, C.A. Miller, J. Butler, M. Ugander, E.B. Schelbert, Extracellular volume and global longitudinal strain both associate with outcomes but correlate minimally, J. Am. Coll. Cardiol. Img. 13 (11) (2020) 2343–2354.
[2] J.J. Park, J.B. Park, J.H. Park, G.Y. Cho, Global longitudinal strain to predict mortality in patients with acute heart failure, J. Am. Coll. Cardiol. 71 (18) (2018) 1947–1957.
[3] S. Romano, R.M. Judd, R.J. Kim, H.W. Kim, I. Klem, J.F. Heitner, D.J. Shah, J. Jue, B.E. White, R. Indorkar, C. Shenoy, A. Farzaneh-Far, Feature-tracking global longitudinal strain predicts death in a multicenter population of patients with ischemic and nonischemic dilated cardiomyopathy incremental to ejection fraction and late gadolinium enhancement, J. Am. Coll. Cardiol. Img. 11 (10) (2018) 1419–1429.

[4] C. Jin, J. Weber, H. Singh, K. Gliganic, J.J. Cao, The association of reduced left ventricular strains with increased extracellular volume and their collective impact on clinical outcomes, J. Cardiovasc. Magn. Reson. 23 (1) (2021) 93.

[5] T. Stanton, R. Leano, T.H. Marwick, Prediction of all-cause mortality from global longitudinal speckle strain: comparison with ejection fraction and wall motion scoring, Circ. Cardiovasc. Imaging 2 (5) (2009) 356–364.

[6] M. Dandel, H. Lehmkuhl, C. Knosalla, N. Suramelashvili, R. Hetzer, Strain and strain rate imaging by echocardiography - basic concepts and clinical applicability, Curr. Cardiol. Rev. 5 (2) (2009) 133–148.

[7] A. Schuster, K.N. Hor, J.T. Kowallick, P. Beerbaum, S. Kutty, Cardiovascular magnetic resonance myocardial feature tracking: concepts and clinical applications, Circ. Cardiovasc. Imaging 9 (4) (2016) e004077.

[8] F. Andre, H. Steen, P. Matheis, M. Westkott, K. Breuninger, Y. Sander, R. Kammerer, C. Galuschky, E. Giannitsis, G. Korosoglou, H.A. Katus, S.J. Buss, Age- and gender-related normal left ventricular deformation assessed by cardiovascular magnetic resonance feature tracking, J. Cardiovasc. Magn. Reson. 17 (2015) 25.

[9] E. Maret, T. Todt, L. Brudin, E. Nylander, E. Swahn, J.L. Ohlsson, J.E. Engvall, Functional measurements based on feature tracking of cine magnetic resonance images identify left ventricular segments with myocardial scar, Cardiovasc. Ultrasound 7 (2009) 53.

[10] M. Barreiro-Perez, D. Curione, R. Symons, P. Claus, J.U. Voigt, J. Bogaert, Left ventricular global myocardial strain assessment comparing the reproducibility of four commercially available CMR-feature tracking algorithms, Eur. Radiol. 28 (12) (2018) 5137–5147.

[11] G. Morton, A. Schuster, R. Jogiya, S. Kutty, P. Beerbaum, E. Nagel, Inter-study reproducibility of cardiovascular magnetic resonance myocardial feature tracking, J. Cardiovasc. Magn. Reson. 14 (2012) 43.

[12] F. Pathan, H.A. Zainal Abidin, Q.H. Vo, H. Zhou, T. D'Angelo, E. Elen, K. Negishi, V.O. Puntmann, T.H. Marwick, E. Nagel, Left atrial strain: a multi-modality, multi-vendor comparison study, Eur. Heart J. Cardiovasc. Imaging (2019).

[13] K. Fischer, O.L. Linder, S.A. Erne, A.W. Stark, S.J. Obrist, B. Bernhard, D. P. Guensch, A.T. Huber, R.Y. Kwong, C. Grani, Reproducibility and its confounders of CMR feature tracking myocardial strain analysis in patients with suspected myocarditis, Eur. Radiol. 32 (5) (2022) 3436–3446.

[14] S.J. Backhaus, G. Metschies, M. Billing, J. Schmidt-Rimpler, J.T. Kowallick, R. J. Gertz, T. Lapinskas, E. Pieske-Kraigher, B. Pieske, J. Lotz, B. Bigalke, S. Kutty, G. Hasenfuss, S. Kelle, A. Schuster, Defining the optimal temporal and spatial resolution for cardiovascular magnetic resonance imaging feature tracking, J. Cardiovasc. Magn. Reson. 23 (1) (2021) 60.

[15] S. Leng, R.S. Tan, X. Zhao, J.C. Allen, A.S. Koh, L. Zhong, Fast long-axis strain: a simple, automatic approach for assessing left ventricular longitudinal function with cine cardiovascular magnetic resonance, Eur. Radiol. 30 (7) (2020) 3672–3683.

[16] J.H. Riffel, F. Andre, M. Maertens, F. Rost, M.G. Keller, S. Giusca, S. Seitz, A. V. Kristen, M. Muller, E. Giannitsis, G. Korosoglou, H.A. Katus, S.J. Buss, Fast assessment of long axis strain with standard cardiovascular magnetic resonance: a validation study of a novel parameter with reference values, J. Cardiovasc. Magn. Reson. 17 (1) (2015) 69.

[17] V. Klinke, S. Muzzarelli, N. Lauriers, D. Locca, G. Vincenti, P. Monney, C. Lu, D. Nothnagel, G. Pilz, M. Lombardi, A.C. van Rossum, A. Wagner, O. Bruder, H. Mahrholdt, J. Schwitter, Quality assessment of cardiovascular magnetic resonance in the setting of the European CMR registry: description and validation of standardized criteria, J. Cardiovasc. Magn. Reson. 15 (1) (2013) 55.

[18] M.S. Nacif, A.D. Barranhas, E. Turkbey, E. Marchiori, N. Kawel, R.A. Mello, R. O. Falcao, A.C. Oliveira Jr., C.E. Rochitte, Left atrial volume quantification using cardiac MRI in atrial fibrillation: comparison of the Simpson's method with biplane area-length, ellipse, and three-dimensional methods, Diagn. Interv. Radiol. 19 (3) (2013) 213–220.

[19] T.K. Koo, M.Y. Li, A Guideline of selecting and reporting intraclass correlation coefficients for reliability research, J. Chiropr. Med. 15 (2) (2016) 155–163.

[20] J.F. Juffermans, S.C.S. Minderhoud, J. Wittgren, A. Kilburg, A. Ese, B. Fidock, Y. C. Zheng, J.M. Zhang, C.P.S. Blanken, H.J. Lamb, J.J. Goeman, M. Carlsson, S. Zhao, R.N. Planken, P. van Ooij, L. Zhong, X. Chen, P. Garg, T. Emrich, A. Hirsch, J. Toger, J.J.M. Westenberg, Multicenter consistency assessment of valvular flow quantification with automated valve tracking in 4D flow CMR, J. Am. Coll. Cardiol. Img. 14 (7) (2021) 1354–1366.

[21] S.L. Ayton, A. Alfuhied, G.S. Gulsin, K.S. Parke, J.V. Wormleighton, J.R. Arnold, A. J. Moss, A. Singh, H. Xue, P. Kellman, M.P.M. Graham-Brown, G.P. McCann, The interfield strength agreement of left ventricular strain measurements at 1.5 T and 3 T using cardiac MRI feature tracking, J. Magn. Reson. Imaging (2022).

[22] J.T. Kowallick, S. Kutty, F. Edelmann, A. Chiribiri, A. Villa, M. Steinmetz, J. M. Sohns, W. Staab, N. Bettencourt, C. Unterberg-Buchwald, G. Hasenfuss, J. Lotz, A. Schuster, Quantification of left atrial strain and strain rate using Cardiovascular Magnetic Resonance myocardial feature tracking: a feasibility study, J. Cardiovasc. Magn. Reson. 16 (1) (2014) 60.

[23] M. Habibi, H. Chahal, A. Opdahl, O. Gjesdal, T.M. Helle-Valle, S.R. Heckbert, R. McClelland, C. Wu, S. Shea, G. Hundley, D.A. Bluemke, J.A. Lima, Association of CMR-measured LA function with heart failure development: results from the MESA study, J. Am. Coll. Cardiol. Img. 7 (6) (2014) 570–579.

[24] B.H. Freed, V. Daruwalla, J.Y. Cheng, F.G. Aguilar, L. Beussink, A. Choi, D.A. Klein, D. Dixon, A. Baldridge, L.J. Rasmussen-Torvik, K. Maganti, S.J. Shah, Prognostic utility and clinical significance of cardiac mechanics in heart failure with preserved ejection fraction: importance of left atrial strain, Circ. Cardiovasc. Imaging 9 (3) (2016).

[25] M.C. Halfmann, S. Altmann, U.J. Schoepf, C. Reichardt, J.B. Hennermann, K.-F. Kreitner, R. Kloeckner, F. Hahn, C. Dueber, A. Varga-Szemes, C. Kampmann, T. Emrich, Left atrial strain correlates with severity of cardiac involvement in Anderson-Fabry disease, Eur. Radiol. 33 (3) (2022) 2039–2051.

[26] S. Leng, R.S. Tan, X. Zhao, J.C. Allen, A.S. Koh, L. Zhong, Validation of a rapid semi-automated method to assess left atrial longitudinal phasic strains on cine cardiovascular magnetic resonance imaging, J. Cardiovasc. Magn. Reson. 20 (1) (2018) 71.

[27] L. Hopman, M.J. Mulder, A.M. van der Laan, P. Bhagirath, A. Demirkiran, M.B. von Bartheld, M.J.B. Kemme, A.C. van Rossum, C.P. Allaart, M.J.W. Gotte, Left atrial strain is associated with arrhythmia recurrence after atrial fibrillation ablation: Cardiac magnetic resonance rapid strain vs. feature tracking strain, Int. J. Cardiol. 378 (2023) 23–31.